

STRUCTURE STUDIES OF POROUS OXIDE LAYERS FORMED ON 13CrMo4-5 STEELS LONG-TERM OPERATED IN THE POWER INDUSTRY

Monika Gwoździk

Faculty of Production Engineering and Materials Technology,
Institute of Materials Engineering
Czestochowa University of Technology

Received 1 June 2016; accepted 6 September 2016; available online 27 September 2016

Key words: 13CrMo4-5 steel, oxide layer, porosity.

Abstract

The paper contains results of studies on the formation of oxide layers on 13CrMo4-5 steel long-term operated at an elevated temperature. The material studied comprised specimens of 13CrMo4-5 steel operated at the temperature of 455°C during 130,000 hours (steel 1) and 540°C during 120,000 hours (steel 2). The oxide layer was studied on a surface and a cross-section at the outer surface of the tube wall. The paper contains results of studies of porosity in the oxide layer. The oxide layer formed on the studied steel 1 is ~146 µm thick, while on the steel 2 ~248 µm. It has been found that steel 2 has higher porosity.

Introduction

At present the huge development in materials engineering has taken place, especially in surface engineering (JAGIELSKA-WIADEREK 2012, KULESZA and BRAMOWICZ 2014, LABISZ 2014, PRISS et al. 2014, SZAFARSKA and IWASZKO 2012). In the previous years a lot of articles were devoted to the topic of steel oxidation (BISCHOFF et al. 2013, CHABIČOVSKÝ et al. 2015, FRANGINI et al. 2014, GRUBER et al. 2015), especially the steel used in power industry. The subject area is connected with oxidation and steel corrosion used in power industry.

Correspondence: Monika Gwoździk, Czestochowa University of Technology, 19 Armii Krajowej Av., 42-200 Częstochowa, Poland, e-mail: gwozdzik@wip.pcz.pl

This topic is widely discussed by a lot of scientific centers in our country and in the world. The research is carried out i.e. on steel such as: 13CrMo4-5, 10CrMo9-10, 16Mo3 and X10CrMoVNb9-1 (ABANG et al. 2011, BANKIEWICZ et al. 2013, GRUBER et al. 2015, GWOŹDZIK 2015, PRISS et al. 2014). The problem of this corrosion, so-called high temperature corrosion is still up to date, i.e. because of modernization and prolonging operation time of existing energetic units. The growth of the oxide layer is accompanied by the growth of numerous defects such as: pores, fissures, flaking. Abang and others in paper (ABANG et al. 2011) conducted the examination i.e. connected with steel oxidation: 16Mo3, 13CrMo4-5 and 10CrMo9-10 during 1100 hours. The researchers showed that dominating oxides are hematite (Fe_2O_3) and magnetite (Fe_3O_4) for these three steels. The researches showed that the created oxide layer is characterized by porosity for these three steels. However, depending on oxidation conditions (air or oxyfuel) and also from oxidation side, porosity is less or more intensified.

Chemical compounds in the flue gas have a strong influence on the formed oxide layers. The service life of components operating in the power industry is highly affected by aggressive components of the flue gases and ashes. Such components cause corrosion of external surfaces of tubes and their corrosion damage. Under normal conditions oxide layers form on the steel surface at the presence of oxygen, making a natural passive layer of steel and a barrier to other gaseous components of the flue gas. However, the situation changes drastically under conditions of oxygen deficiency and at the moment of accumulation of thick deposit layers on the tube surface. This happens because physicochemical parameters under the deposits substantially differ from those existing in the flowing flue gas stream and then – depending on the chemical composition of the formed deposits and on their morphology – to a varying extent they can aggressively influence the steel and protective layers. The high-temperature corrosion threat may be higher or smaller, depending on the fuel type. Acc. to authors (GAWRON and KLEPACKI 2012) the high-temperature corrosion threat to boiler heatable surfaces increases under conditions of low-emission combustion with a share of alternative fuels.

The aim of the paper was conducting the examination connected with the structure studies of porous oxide layers created on 13CrMo4-5 steel operated in different temperature-time conditions.

Material and Experimental Methods

The material studied comprised specimens of 13CrMo4-5 (15HM) steels long-term operated at an elevated temperature:

- steel 1, T = 455°C, t = 130,000 h,
- steel 2, T = 540°C, t = 120,000 h.

The oxide layer was studied on a surface and a cross-section at the outer surface of the tube wall (Fig. 1).

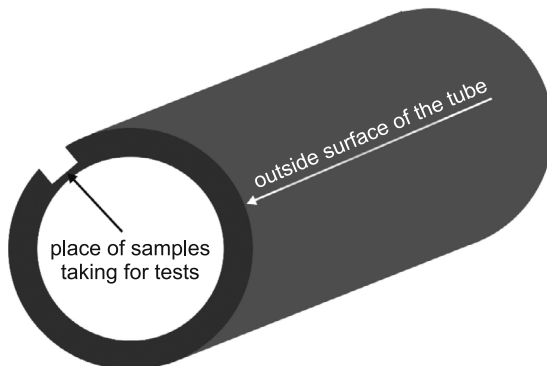


Fig. 1. Place of samples taking for tests

Thorough examinations of the oxide layer carried out on the outer surface wall of tube wall comprised:

- the analysis of steel chemical composition was carried out using spark emission spectroscopy on a Spectro spectrometer (Table 1),
- macroscopic and microscopic examinations of the oxide layer were performed using an Olympus SZ61, GX41 optical microscope and Jeol JSM-6610LV scanning electron microscope (SEM),
- thickness measurements of formed oxide layers,
- chemical composition analysis of deposits/oxides using a Jeol JSM-6610LV scanning electron microscope (SEM) working with an Oxford EDS electron microprobe X-ray analyser,
- X-ray (XRD) measurements; the layer was subject to measurements using a Seifert 3003T/T X-ray diffractometer and the radiation originating from a tube with a cobalt anode ($\lambda_{Co} = 0.17902$ nm). A computer software and the DHN PDS, PDF4+2009 crystallographic database were used for the phase identification.

Table 1
Chemical composition of examined steel, wt %

Acc.	Chemical composition, wt %						
	C	Si	Mn	P	S	Cr	Mo
Analysis (steel 1)	0.16	0.30	0.57	0.019	0.009	0.90	0.54
Analysis (steel 2)	0.09	0.31	0.47	0.014	0.007	0.91	0.52
PN-EN 10028-2	0.08-0.18	max. 0.35	0.40-1.00	max. 0.025	max. 0.010	0.70-1.15	0.40-0.60

Results of examinations

Steels 1 and 2 have the same structure, which is ferrite, perlite and bainite (Fig. 2). For steel 1 it was observed that the size of the grain is diversified and the elements of the structure are unequally placed. In addition, in this steel there are sporadic sulphide precipitates which occur both inside and on the grain boundaries (Fig. 2a). The structure of steel 2 is characterized by a large amount of carbide precipitates both inside and on the grain boundaries. The carbides which occur on the grain boundaries create so-called "chains" (Fig. 2b).

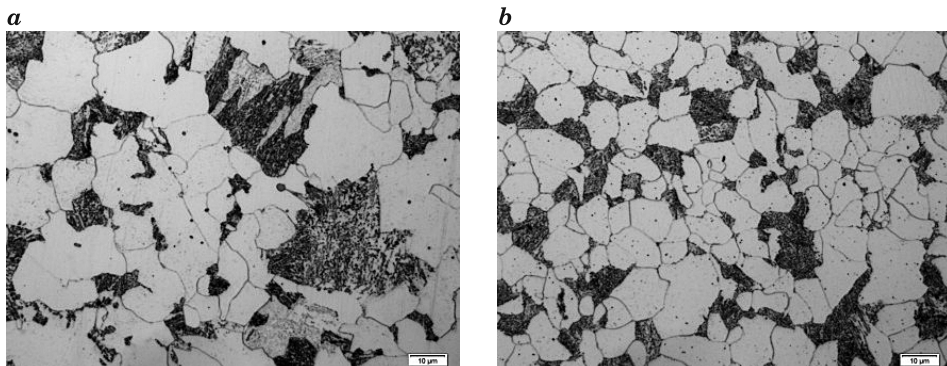


Fig. 2. Microstructure of 13CrMo4-5 steel, LM, 1000x: a – steel 1, b – steel 2

The macroscopic observation of the examined surfaces (Fig. 3) showed that in both cases the significant development level of the surfaces and the outer layer damages occur.

Observations of the oxide layer surface by means of scanning electron microscopy have shown that in the case of steel 1 there are oxide areas without damage, presented in Fig. 4a. In turn, Fig. 4b presents a damaged oxide layer from the same steel. Damaged areas of the layer, which are crystalline in nature, are visible. Figs. 4c and d present the oxide surface formed on steel 2. A significant surface development may be observed on this steel. Also deposits exist, apart from the oxide layer, confirmed by the EDS analysis (Fig. 5).

Performed XRD measurements (Fig. 6) have shown that in both cases (steel 1 and 2) the oxide layer is built of hematite (Fe_2O_3) and magnetite (Fe_3O_4). Moreover, the EDS analysis in both cases have shown the existence of Si and additionally – for steel 2 – of Al. These elements form such compounds as SiO_2 and Al_2O_3 , which are components of hard coal ashes.

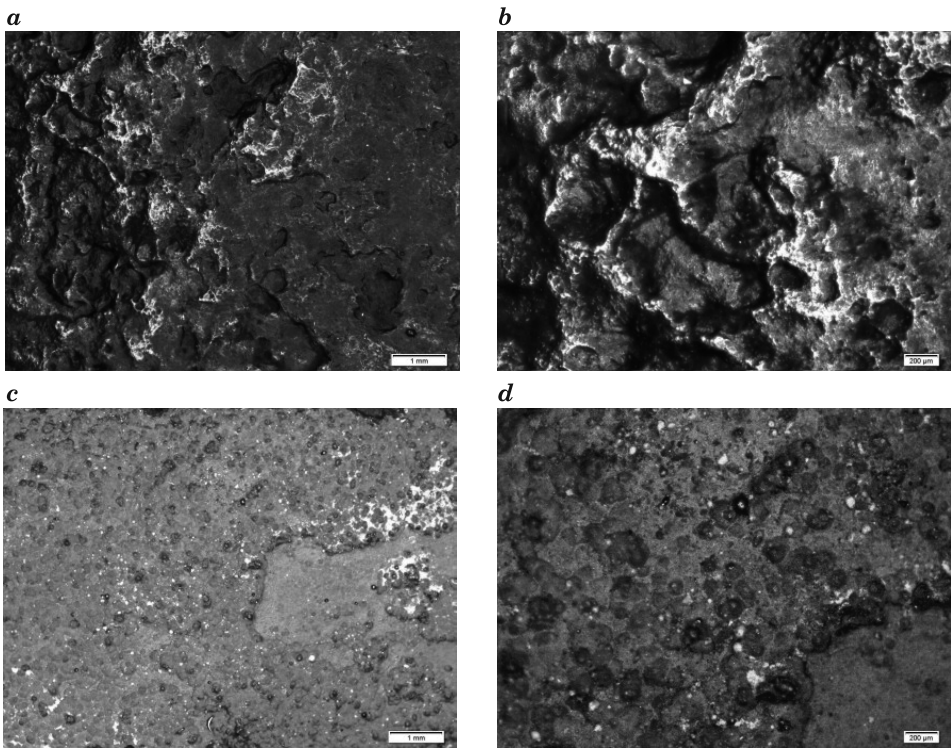


Fig. 3. Oxides formed on 13CrMo4-5 steel, outer surface, LM: *a* – steel 1, 15x, *b* – steel 1, 45x, *c* – steel 2, 15x, *d* – steel 2, 45x

Observations of metallographic microsections made on a cross-section have shown that for steel 1 the oxide layer was ~ 146 μm thick (Fig. 7a), while for steel 2 it was 100 μm thicker and was ~ 248 μm (Fig. 7b).

In the case of steel 1 (Fig. 8) the amount of defects in the formed layer is much smaller than for steel 2 (Fig. 9). The oxide layer formed on steel 1 shows local damage in the form of numerous cracks, which locally create a network on the entire layer cross-section (Fig. 8a, b). Large fissures originate in places and fine porosity exists locally. In turn steel 2 features a great degradation (Fig. 9). In some places the oxide layer is entirely separated from the substrate, which is shown in Fig. 9a. Also huge fissures occur, reaching the depth of 70 μm (Fig. 9b). The oxide layer on steel 2 is mostly torn off and cracked (Fig. 9c). In addition, in steel 2 directly on the steel side there is major corrosion along grain boundaries, reaching the depth of 15 μm (Fig. 10). Abang and others in paper (ABANG et al. 2011) showed that, under both operating conditions the surface layer was characterised by loosely attached formations of ash that were partially flaked. The outer layer of corrosion was covered with many tiny pores. Apart from the tiny pores under oxyfuel conditions, the inner layer of corrosion also had a few large pores.

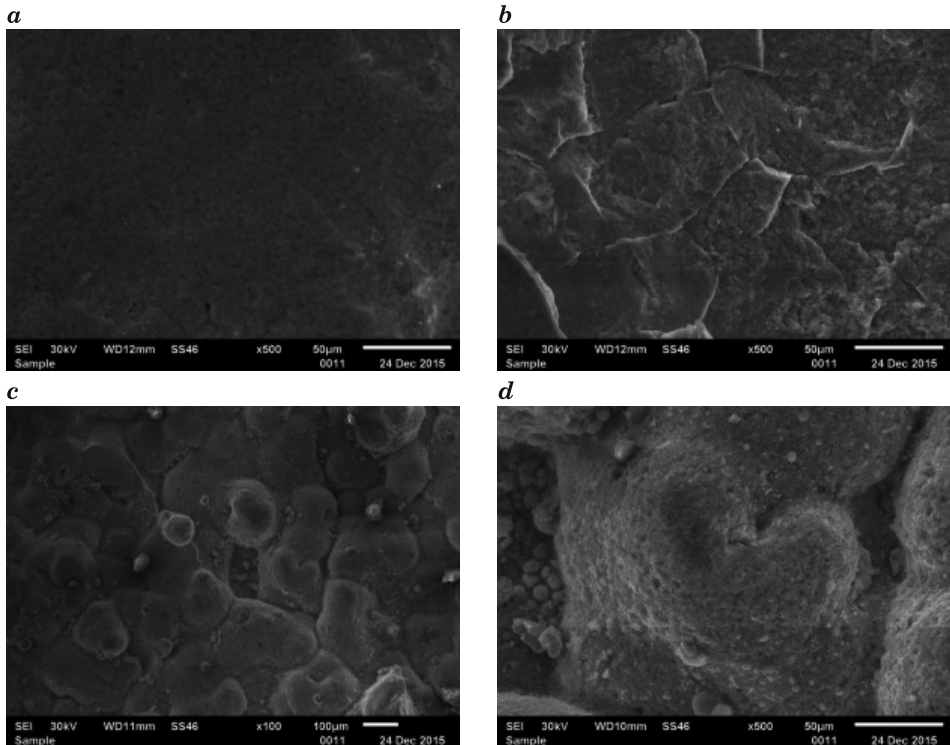


Fig. 4. Oxides formed on 13CrMo4-5 steel, outer surface, SEM: a, b – steel 1, 500x, c – steel 2, 100x, d – steel 2, 500x

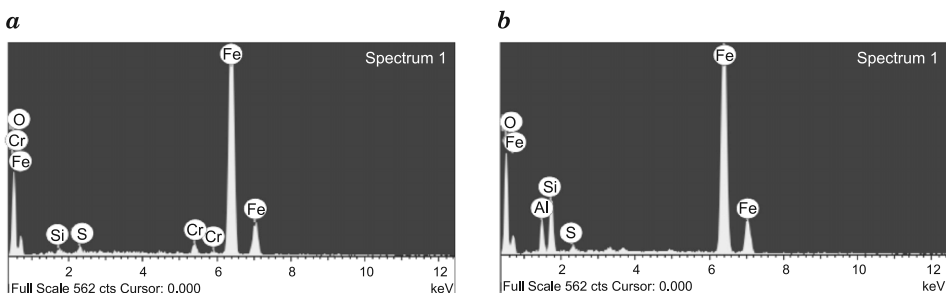


Fig. 5. SEM / EDS: a – steel 1, b – steel 2

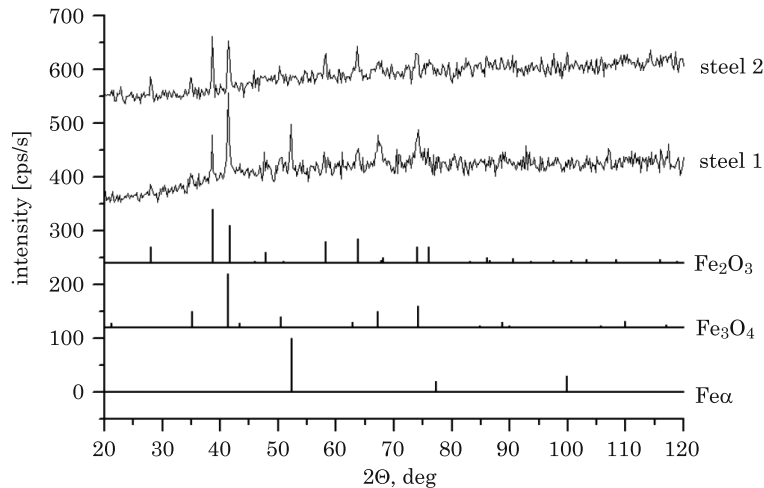


Fig. 6. X-ray diffraction patterns from the oxides layer obtained by means of XRD technique

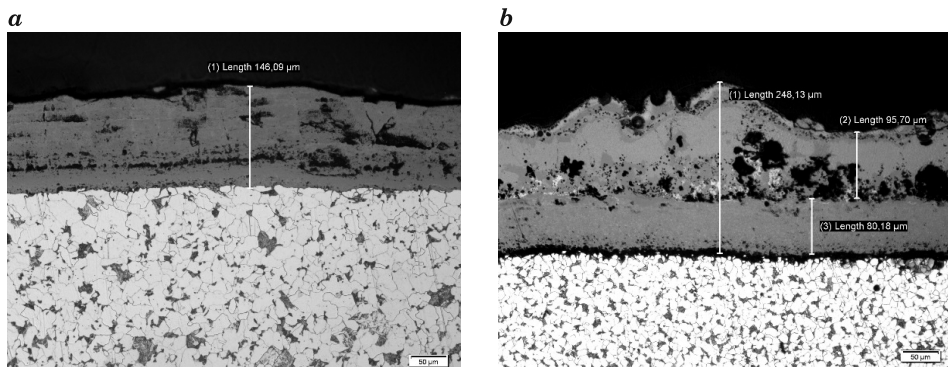


Fig. 7. The thickness of oxide layer formed on the steel examined, LM, 200x: a – steel 1, b – steel 2

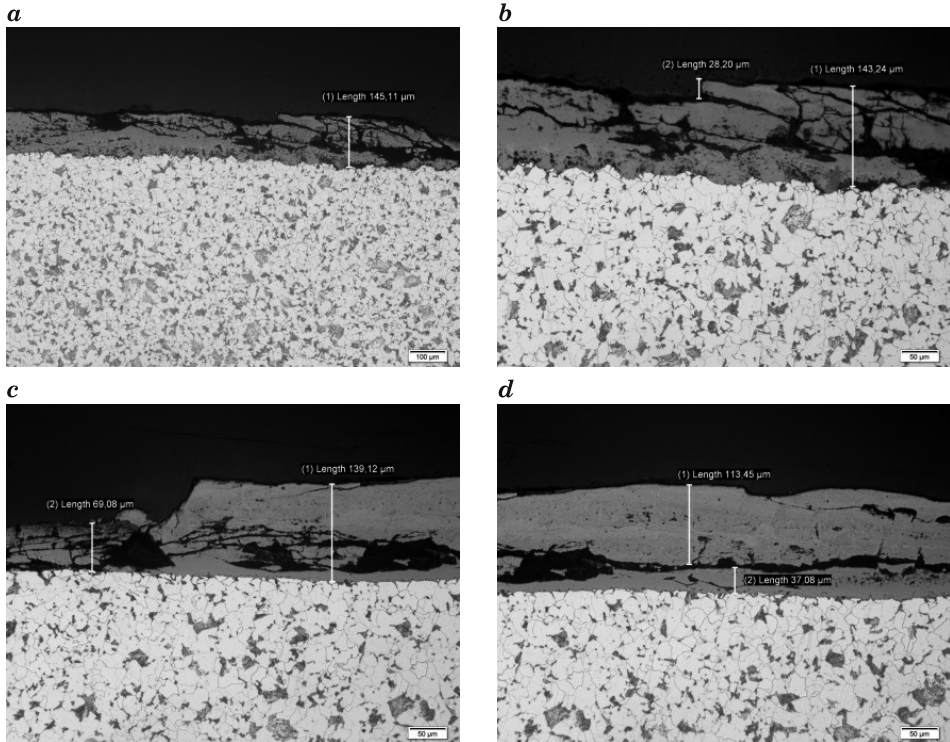


Fig. 8. Defects of oxides layer existing on steel 1

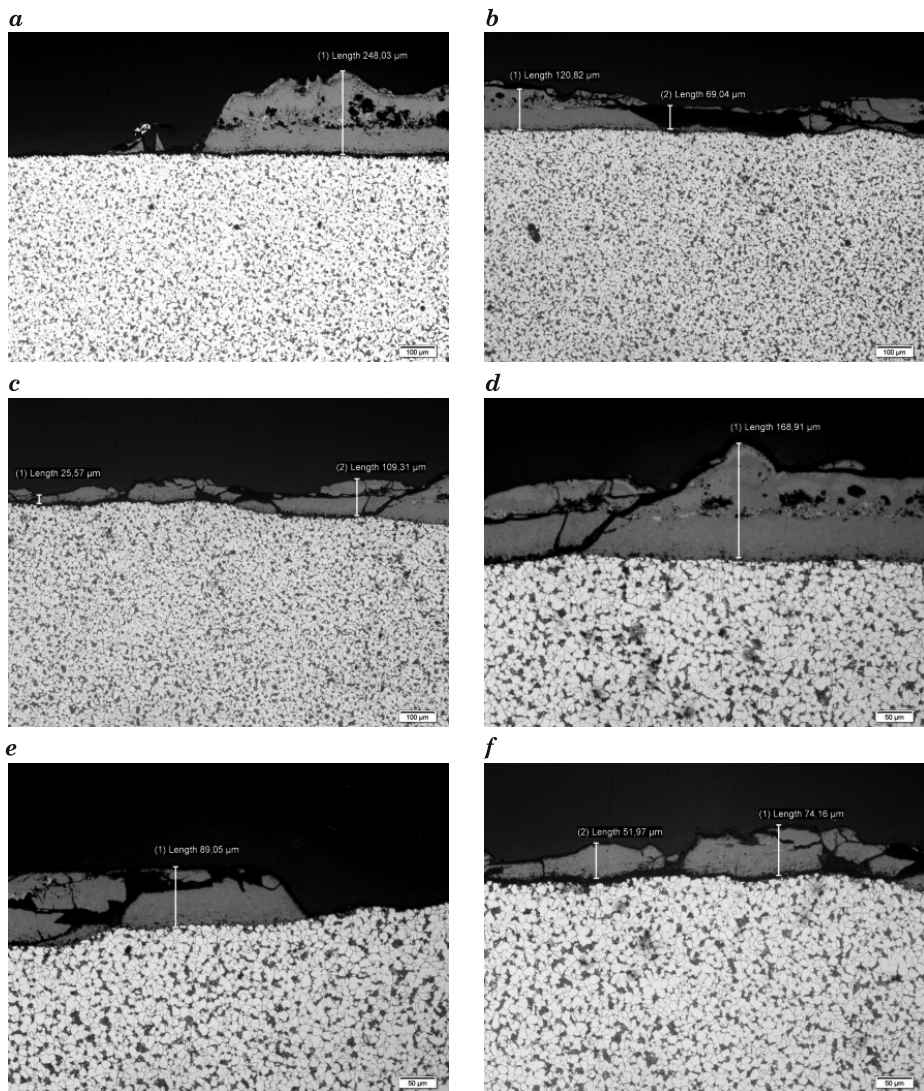


Fig. 9. Defects of oxides layer existing on steel 2

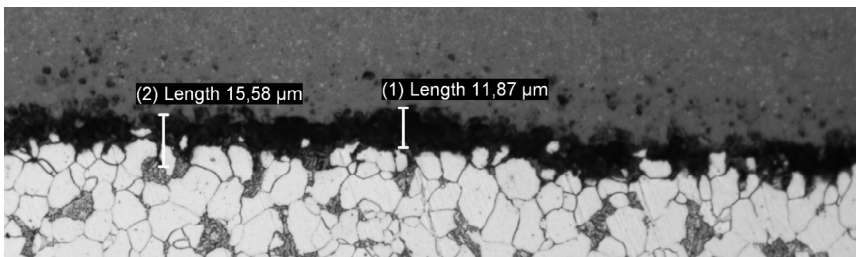


Fig. 10. Corrosion on the grain boundaries at the outside surface, 500x

Summary

The obtained results of studies have shown that porosity exists in the oxide layer formed on both steels. When observing a continuous oxide layer (without spalling) it is possible to notice that the porosity is situated mainly on the flue gas inflow side. Much larger pores were observed for steel 2 than for steel 1, which is visible in Fig. 7. Instead, photographs of areas covered by major degradation show numerous cracks and spalling cases of the oxide layer, resulting from such defects of the structure as numerous pores, which then transform into fissures. Areas of spalling covering in places the entire cross-section of the oxide layer thickness were observed for steel 2. The results of studies for steel 13CrMo4-5 have shown that during a component operation at a higher temperature the oxide layer is degraded to a greater degree.

References

- ABANG R., FINDEISEN A., KRAUTZ H.J. 2011. *Corrosion behaviour of selected power plant materials under oxyfuel combustion conditions*. Górnictwo i Geoinżynieria, 35(3/1): 23–42.
- BANKIEWICZ D., YRJAS P., LINDBERG D., HUPA M. 2013. *Determination of the corrosivity of Pb-containing salt mixtures*. Corrosion Science, 66: 225–232.
- BISCHOFF J., MOTTA A.T., EICHFELD C., COMSTOCK R.J., CAO G., ALLEN T.R. 2013. *Corrosion of ferritic-martensitic steels in steam and supercritical water*. Journal of Nuclear Materials, 441: 604–611.
- CHABIČOVSKÝ M., HNÍZDIL M., TSENG A.A., RAUDENSKÝ M. 2015. *Effects of oxide layer on Leidenfrost temperature during spray cooling of steel at high temperatures*. International Journal of Heat and Mass Transfer, 88: 236–246.
- EN 10028-2:2009: *Flat products made of steels for pressure purposes – Part 2: Non-alloy and alloy steels with specified elevated temperature properties*.
- FRANGINI S., MASCI A., MCPHAIL S.J., SOCCIO T., ZAZA F. 2014. *Degradation behavior of a commercial 13Cr ferritic stainless steel (SS405) exposed to an ambient air atmosphere for IT-SOFC interconnect applications*. Materials Chemistry and Physics, 144: 491–497.
- GAWRON P., KLEPACKI F. 2012. *Trwałość wybranych elementów kotłów w warunkach współspalania biomasy*. Energetyka, 6(696): 293–303.
- GRUBER T., SCHARLER R., OBERNBERGER I. 2015. *Application of an empirical model in CFD simulations to predict the local high temperature corrosion potential in biomass fired boilers*. Biomass and Bioenergy, 79: 145–154.
- GWOŹDZIK M. 2015. *Characterization of Oxide Layers Formed on 13CrMo4-5 Steel Operated for a Long Time at an Elevated Temperature*. Archives of Metallurgy and Materials, 60(3A): 1783–1788.
- JAGIELSKA-WIADEREK K. 2012. *Depth-profiles of corrosion properties of carbonitrided AISI 405 steel*. Archives of Metallurgy and Materials, 57(2): 637–642.
- KULESZA S., BRAMOWICZ M. 2014. *A comparative study of correlation methods for determination of fractal parameters in surface characterization*. Applied Surface Science, 293: 196–201.
- LABISZ K. 2014. *Microstructure and mechanical properties of high power diode laser (HPDL) treated cast aluminium alloys*. Mat.-wiss. U. Werkstofftech, 45(4): 314–324.
- PRISS J., ROJACZ H., KLEVTSOV I., DEDOV A., WINKELMANN H., BADISCH E. 2014. *High temperature corrosion of boiler steels in hydrochloric atmosphere under oil shale ashes*. Corrosion Science, 82: 36–44.
- SZAFARSKA M., IWASZKO J. 2012. *Laser remelting treatment of plasma-sprayed Cr₂O₃ oxide coatings*. Archives of Metallurgy and Materials, 57(1): 215–221.